Society For Biomaterials

A comparative study of polyethylene glycol hydrogels derivatized with the RGD peptide and the cell-binding domain of fibronectin

Chen Zhang, Sogol Hekmatfer, Nancy W. Karuri

Department of Chemical and Biological Engineering, Illinois Institute of Technology, Chicago, Illinois 60616

Received 5 October 2012; revised 4 February 2013; accepted 21 February 2013
Published online 24 April 2013 in Wiley Online Library (wileyonlinelibrary.com). DOI: 10.1002/jbm.a.34687

Abstract: The goal of our study was to compare the biological responses of cells cultured on polyethylene glycol (PEG) hydrogels functionalized with varying concentrations of the widely used adhesion peptide, RGD, and the cell-binding domain of fibronectin, $III_{9\text{-}10}$. We used Michael addition chemistry to covalently link cysteines in GRGDSPC and glutathione *S*-transferase (GST) tagged $III_{9\text{-}10}$ (GST-$III_{9\text{-}10}$), to the acrylate groups in PEG diacrylate (PEGDA). Conjugation of GST-$III_{9\text{-}10}$ to PEGDA occurred through cysteine residues in GST. Ellman's reagent and immunoblotting studies demonstrated an efficiency of 90% or more for PEG conjugation of 1 μM GST-$III_{9\text{-}10}$ or GRDGSPC in 10% (wt/vol) PEGDA at 37°C for 1 h. Circular dichroism and limited proteolysis demonstrated that conjugating PEGDA to GST-$III_{9\text{-}10}$ did not significantly perturb its native secondary structure. Sodium dodecyl sulfate polyacrylamide gel electrophoresis characterization of the wash solution of PEG hydrogels after photopolymerization demonstrated that >95% of the 1 μM GST-$III_{9\text{-}10}$ was incorporated into the PEG hydrogels after cross-linking. PEG hydrogels derivatized with 1 μM GST-$III_{9\text{-}10}$ had significantly higher cell adhesion and spreading than PEG hydrogels with 1 μM GRGDSPC. A comparable adhesion response between GRGDSPC and GST-$III_{9\text{-}10}$ was obtained when the former was at millimolar and the latter at micromolar concentration. The amount and type of conjugate in the PEG hydrogel derivative was statistically more significant than hydrogel rigidity in stimulating the biological responses observed. This report presents new evidence of the robustness of $III_{9\text{-}10}$ in mediating cell adhesion and spreading on PEG hydrogels. © 2013 Wiley Periodicals, Inc. J Biomed Mater Res Part A: 102A: 170–179, 2014.

Key Words: cell-binding domain, fibronectin, polyethylene glycol hydrogel, cell adhesion, spreading, rheology

How to cite this article: Zhang C, Hekmatfer S, Karuri NW. 2014. A comparative study of polyethylene glycol hydrogels derivatized with the RGD peptide and the cell-binding domain of fibronectin. J Biomed Mater Res Part A 2014:102A:170–179.

INTRODUCTION

The extracellular matrix (ECM) provides physical and chemical cues that direct tissue growth and development. It is composed of proteins and polysaccharides. In many soft tissues, it is a fibrillar and highly hydrated scaffold. Polyethylene glycol (PEG) hydrogels are cross-linked hydrated polymers that are biologically inert. Synthetic ECM analogs based on composites of ECM molecules and PEG hydrogels are desirable for tissue engineering applications because they physically and chemically mimic the ECM. Furthermore, the quantity and organization of the biologically active molecules immobilized on these synthetic analogs can be varied to obtain favorable cellular and tissue responses.[1]

PEG hydrogels conjugated to the RGD tripeptide, which is found in ECM proteins such as fibronectin, support cell adhesion and migration, bone mineralization, and protein expression.[2–4] RGD is part of an exposed loop on the surface of the tenth type III repeat of fibronectin, III_{10}. RGD has a synergy site in III_9.[5,6] The structure of the interface between RGD and its synergy site influences cell attachment and spreading.[7,8] Recent studies have suggested that conjugation of the cell-binding domain of fibronectin, $III_{9\text{-}10}$, to synthetic scaffolds results in a more robust and selective biological response in cells than conjugation of RGD-based peptides.[7–11] However, there are no quantitative studies comparing the effect of different amounts of $III_{9\text{-}10}$ and RGD conjugated to PEG hydrogel networks on cellular responses. These studies are important because of the wide use of PEG hydrogels as ECM mimics.[1,11,12] Moreover, cells respond to scaffold rigidity, which may be influenced by bioconjugates in the PEG hydrogel network.[13]

The most commonly used approaches to conjugate PEG molecules to proteins involve forming covalent bonds with (i) thiols in cysteine residues or (ii) primary amines in lysine residues or in the amino terminal end of the molecule. $III_{9\text{-}10}$ has 10 lysines and no cysteines.[6] Cosson et al.[12] biotinylated primary amines in $III_{9\text{-}10}$ and then attached them to the surface of PEG hydrogels functionalized with gradients of NeutrAvidin to modulate cell migration. Conjugating $III_{9\text{-}10}$ to the polymer network via multiple amines in lysine residues has the potential to influence important binding interactions if the presence of PEG sterically inhibits

Correspondence to: N. W. Karuri; e-mail: nkaruri1@iit.edu

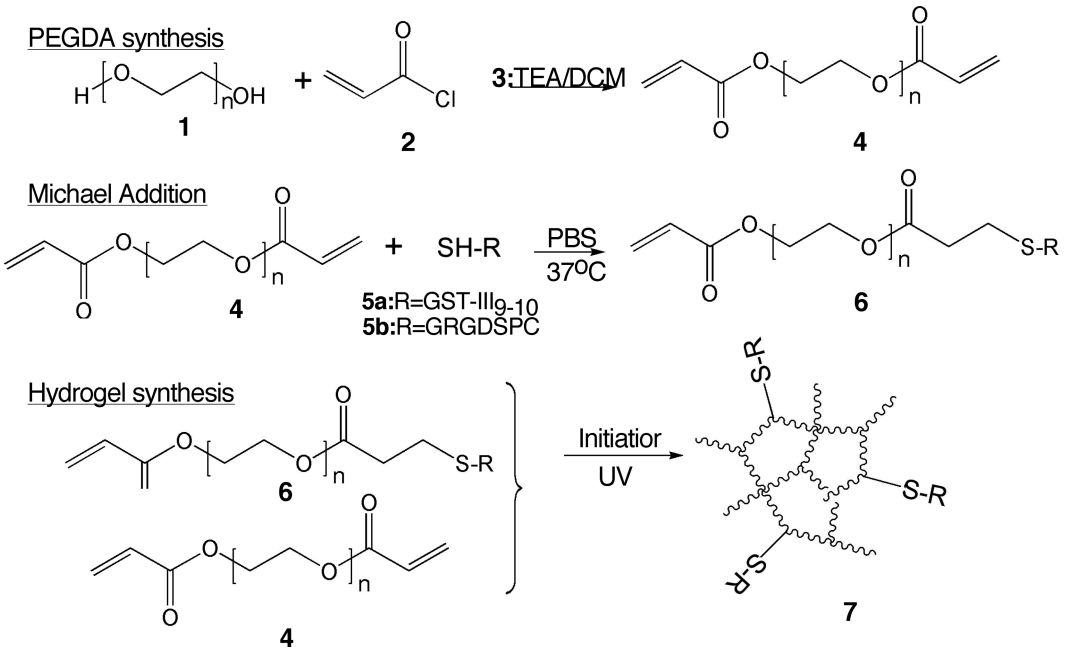

FIGURE 1. Schematic of the synthesis of PEG hydrogels functionalized with GST-III_{9-10} and GRGDSPC. PEG macromers (**1**) were reacted with acryloyl chloride (**2**) in the presence of TEA and DCM (**3**) to form PEGDA (**4**) GST-III_{9-10} or GRGDSPC (**5a** and **5b,** respectively) were covalently bonded to PEGDA (**4**) to form the PEG-conjugated macromers (**6**). PEG conjugation was performed in PBS at 37°C for 1 h. Derivatized PEG hydrogels (**7**) were obtained after photopolymerization of **4** and **6** in the presence of an initiator.

a binding partner. Ghosh et al.[11] addressed the challenge of conjugating PEG to III_{9-10} on cysteine residues by using recombinant DNA technology to introduce a cysteine residue to the amino terminal of III_{9-10} and then covalently cross-linking the cysteine residue to PEG diacrylate (PEGDA). They then covalently cross-linked the PEG conjugated III_{9-10} to thiol-functionalized hyaluronan hydrogels and demonstrated higher migration of fibroblasts on hyaluronan hydrogels with III_{9-10} than those with RGD. The approach by Ghosh et al. was more selective than the approach of Cosson et al. and minimized the risk of steric hindrance caused by conjugating PEG to surface lysine in III_{9-10}. However, their strategy is laborious because it entails multiple processing steps.

The major contribution of this study is the characterization of cell responses on varying quantities of RGD and III_{9-10} on PEG hydrogels. Our approach of conjugating PEG to III_{9-10} takes advantage of a significant difference between the amino acid composition of glutathione *S*-transferase (GST), a fusion protein used in affinity chromatography to purify proteins from bacteria, and III_{9-10}; III_{9-10} has no cysteine residues,[6] whereas GST has three.[14] This feature allows the use of Michael addition chemistry to conjugate PEGDA to cysteine residues in a fusion of GST and III_{9-10}, GST-III_{9-10}, thereby immobilizing III_{9-10}. To the best of our knowledge, this is the first study of its kind that has used GST to tether a protein to PEG. Michael addition occurs efficiently at physiological temperature and pH and is more selective for thiols than amines.[15,16] We demonstrate efficient conjugation of PEG to GST-III_{9-10} and GRGDSPC in a single reaction step. We show that GST-III_{9-10} conjugated to PEG does not differ structurally from GST-III_{9-10} through circular dichroism (CD) and limited proteolysis. We demonstrate that on a molar basis PEG hydrogels covalently bonded with GST-III_{9-10} have significantly higher cell adhesion and spreading than PEG hydrogels with RGD. We show that cells are more sensitive to differences in bioconjugate chemistry in the polymer network of PEG hydrogels than differences in the rigidity of PEG hydrogels caused by the presence of the bioconjugates. The set of approaches for III_{9-10} immobilization that we present is rapid, easy to implement, robust, and produces a well-defined material chemistry on which cell responses can be directed.

MATERIALS AND METHODS

Synthesis and characterization of PEGDA

PEGDA was synthesized using the procedure of Elbert and Hubbell[17] and is described as follows. We used commercially available PEG with a molecular weight range of 3015–3685 Da (**1**) **(**Fig. 1) (Sigma-Aldrich, St Louis, MO). Acryloyl chloride (**2**) (Sigma–Aldrich) and triethylamine (**3**) (TEA; Sigma-Aldrich) were added dropwise to a PEG solution of 0.001 mol/mL in anhydrous dichloromethane (DCM; Sigma-Aldrich). The molar ratio of PEG to TEA to acryloyl chloride was 1:2:4, and the reaction was performed overnight at room temperature. The resulting solution was mixed with potassium carbonate (MP Biomedicals, Solon, OH) and vigorously shaken. The organic phase containing PEGDA (**4**) was collected, precipitated in cold diethyl ether (Thermo Fisher Scientific, Waltham, MA) and dried under vacuum. The acrylation of PEG was confirmed by the presence of characteristic acrylate peaks at 5.8, 6.1, and 6.4 ppm in 1^H NMR

($CDCl_3$) spectra in an Avance Bruker model AQS 300 MHz spectrometer (Bruker BioSpin Corporation, Billerica, MA). The acrylate conversion was calculated to be 93.3% using the method of Cruise et al.[18] and is comparable to that obtained by other groups.[15,18,19]

Conjugation of PEGDA to GST-III$_{9\text{-}10}$ and GRDGSPC and its characterization

GST-III$_{9\text{-}10}$ was isolated by GST-affinity chromatography of bacterial lysates encoding the protein and characterized.[20,21] GRGDSPC was obtained from a commercial source (American Peptide Co., Sunnyvale, CA). Michael addition was used to conjugate thiols in GST-III$_{9\text{-}10}$ or GRGDSPC [Fig. 1.5(a,b)] to acrylates in PEGDA (Fig. 1.6). For this reaction, GRGDSPC or GST-III$_{9\text{-}10}$ at a concentration of 2–20 μ*M* was mixed with an equal volume of 20% (w/v) PEGDA solutions in phosphate-buffered solution (PBS; Fisher Scientific, Pittsburgh, PA).

The extent of conjugation of PEGDA to III$_{9\text{-}10}$ or GRGDSPC was followed by monitoring the consumption of free thiols with Ellman's reagent (Pierce, Rockford, IL). Ellman's reagent reacts with free thiol groups to produce a colored reagent that absorbs light strongly at 412 nm. We generated standard curves of cysteine-hydrochloride monohydrate (Sigma-Aldrich), GST-III$_{9\text{-}10}$, and GRGDSPC in PBS with concentrations ranging from 0 to 16 μ*M* in a UV-VIS spectrophotometer (Shimadzu UV-2401 PC, Japan). We obtained a linear relationship between cysteine concentration and absorbance from these three molecular species. Then, at regular time intervals after the addition of PEGDA to GST-III$_{9\text{-}10}$ or GRGDSPC, aliquots were withdrawn, added to Ellman's reagent, and absorbance at 412 nm was recorded. Absorbance was then converted to thiol concentration. The disappearance of free thiols was monitored for 20 min after mixing the reactants.

An end-point analysis of the products of the reaction between GST-III$_{9\text{-}10}$ and PEG was performed by sodium dodecyl sulfate polyacrylamide gel electrophoresis (SDS-PAGE) and immunoblotting. An hour after mixing, the products of the Michael addition between PEGDA and GST-III$_{9\text{-}10}$ were mixed with electrophoresis sample buffer containing 6.6% sodium dodecyl sulfate (Fisher Scientific), 33.3% glycerol (Fischer Scientific), and 3.3% dithiothreitol (Fisher Scientific). The Michael addition mixture was separated on an 8% polyacrylamide gel, transferred to nitrocellulose membrane, and probed with 7.1 (Developmental Studies Hybridoma Bank, Iowa city, IA). 7.1 is a monoclonal antibody that binds III$_{9\text{-}10}$ and was used at a dilution of 1:1000. The nitrocellulose membrane was then incubated with goat anti-mouse IgG (H+L) horseradish peroxidase conjugates (Invitrogen, Carlsbad, CA) at a dilution of 1:5000 for 1 h. Antibody labeling was detected with SuperSignal West Pico chemiluminescent reagents (Thermo Fisher Scientific Inc.) and imaged by a ChemiDoc^{TM} XRS+ system (Bio-Rad, Hercules, CA).

Proteolysis

Limited proteolysis of GST-III$_{9\text{-}10}$ and PEG-conjugated GST-III$_{9\text{-}10}$ [Fig. 1.5(a) and 1.6] was conducted with α chymotrypsin (Sigma-Aldrich) to determine whether there were changes in the accessibility of proteolytic sites after PEG conjugation. GST-III$_{9\text{-}10}$ and PEGDA were incubated for half an hour at 37°C as described above and dialyzed in PBS. α Chymotrypsin in 100 m*M* Tris-HCl and 10 m*M* $CaCl_2$ at pH 7.8 was added. The mass ratio of α chymotrypsin to GST-III$_{9\text{-}10}$ was 1:10. Proteolysis was performed for 10 min then stopped with 1 m*M* phenylmethanesulfonyl fluoride (Sigma-Aldrich). The products of proteolysis were electrophoresed on an 8% polyacrylamide gel and silver stained using standard techniques. The native protein was used as a control.

CD studies of GST-III$_{9\text{-}10}$ and GRGDSPC conjugated to PEG

CD studies were conducted to determine the secondary structure of native and PEG-conjugated GST-III$_{9\text{-}10}$. GST-III$_{9\text{-}10}$ conjugated to PEG was obtained by mixing 2–20 μ*M* GST-III$_{9\text{-}10}$ and 2–20% (w/v) PEGDA and incubating at 37°C for 1 h. The proteins conjugated to PEG were dialyzed to remove unconjugated PEGDA, and the protein concentration determined by monitoring the absorbance of the proteins at 280 nm. CD spectra of native and PEG-conjugated GST-III$_{9\text{-}10}$ were collected between 190 and 300 nm in a J715 spectropolarimeter (Jasco, Easton, MD). We used a 0.1-cm path length, a temperature of 25°C, a bandwidth of 5 nm, and a scan rate of 100 nm/min to obtain the CD spectra. Five scans were averaged for each individual sample.

Hydrogel preparation

After Michael addition, the products were immediately cross-linked into a hydrogel (Fig. 1.7). This was performed by adding 0.5% (vol/vol) of the initiator 2-hydroxy-2-methylpropiophenone (Sigma-Aldrich) to a solution consisting of PEG-GST-III$_{9\text{-}10}$ or PEG-GRGDSPC and PEGDA. The resulting solution was injected into a 1-mm spacer mold and exposed to UV light (365 nm) for 5 min to form hydrogels. Hydrogels were released from the mold, immersed in PBS solution, and stored at 4°C overnight to remove any traces of the initiator. The wash solution was collected and concentrated 40 times in ultra centrifugal filters with a 10,000 molecular weight cut off (Millipore, Billerica MA). GST-III$_{9\text{-}10}$ in the concentrated wash was analyzed by immunoblotting. PEG hydrogels were cut into 8-mm diameter cylinders using a hole punch and placed into the wells of a 24-well culture plate for cell-based assays.

Cell adhesion assay

The adhesive response of cells to PEG hydrogels derivatized with different amounts of GST-III$_{9\text{-}10}$ and GRGDSPC was determined. Round hydrogel samples of 8-mm diameter were placed into a 24-well culture plate. Each 8-mm piece was incubated with 1% (wt/vol) bovine serum albumin (Sigma-Aldrich) in PBS for 30 min at 37°C to block nonspecific adsorption. The samples were then washed three times with PBS before the addition of cells. NIH 3T3 mouse embryonic fibroblasts (ATCC, Manassas, VA) between passages 21 and 28 were used. The cells were cultured in Dulbecco's

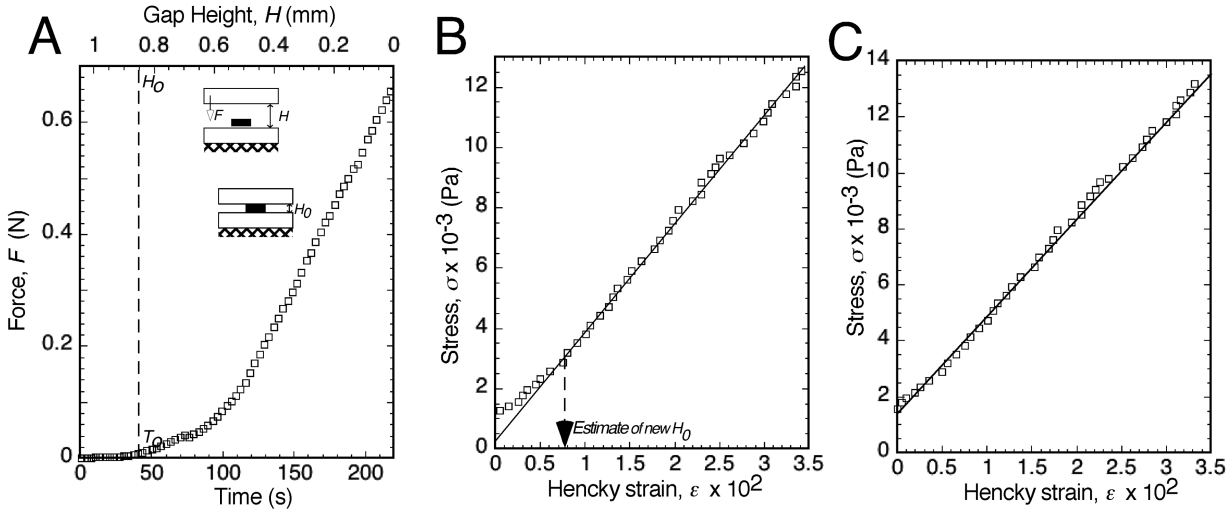

FIGURE 2. Schematic of PEG hydrogel rheology. (A) PEG hydrogel samples were placed on the lower plate of a rheometer and compressed by moving the upper plate (inset). The force–time relationship was used to estimate H_0 the point at which the PEG hydrogel was in contact with the plate. (B) A stress–strain curve was obtained, and a new H_0 was determined from the onset of the linear region. The new H_0 was used to determine a new stress–strain relationship from the data in (A). The final stress–strain relationship was obtained when the stress–strain relationship was linear.

modified eagle's medium (DMEM; Fisher Scientific) supplemented with 10% bovine calf serum (Fisher Scientific) at 37°C and in 5% CO_2. The cells were grown to 80–90% confluence in 10-cm dishes and then trypsinized with 1 mg/mL of TPCK trypsin (Fisher Scientific) in 0.01% ethylenediaminetetraacetic acid (Fisher Scientific) for 5 min at room temperature. Trypsin was inactivated by adding 0.5 mg/mL soybean trypsin inhibitor (Fisher Scientific) in PBS. The cells were isolated by centrifugation and resuspended in serum-free DMEM solution. They were then added to 24-well plates containing PEG hydrogels. Cells were plated at a density of 1×10^5 cells per well and then incubated for 1 h at 37°C with 5% CO_2. After incubation, the samples were washed twice with PBS, fixed with 3.7% paraformaldehyde (Fisher Scientific) in PBS, and permeabilized with 0.5% NP-40 (Fisher Scientific) in PBS. The samples were then rinsed twice with PBS and stained with fluorescein phalloidin (Invitrogen) and Hoechst 33258 (Fisher Scientific). Fluorescein phalloidin and Hoechst 33258 were used at a dilution of 1:50 and a concentration of 1 μg/mL, respectively. Staining was performed in 2% ovalbumin (Sigma-Aldrich) in PBS at 37°C for 45 min. The samples were finally washed three times with PBS and imaged.

Fluorescence microscopy and image analysis

A Carl Zeiss LSM 510 microscope (Carl Zeiss, Thornwood, NY) was used to collect images of the fluorescein and Hoechst stains. The image capture software, Axiovision (Carl Zeiss), a Hoechst filter, and a 10× objective were used to evaluate cell count. Nine areas per sample were counted. A 20× objective was used to capture images under a fluorescein filter for cell spreading. These images were then analyzed to determine cell spreading for at least 20 cells per sample. Image J software (National Institutes of Health) was used to collect the pixelated area of fluorescein fluorescence. The pixilated area was then converted to μm^2 by using the scaling generated by the image capture software.

PEG hydrogel rheology

The mechanical properties of PEG hydrogel samples were measured by biaxial compression between parallel plates.[22,23] A cylindrical hydrogel sample with a (nominal) thickness, H_0, of 1.0 mm and diameter, D_0, of 8.0 mm was placed on the center of the lower plate of a parallel plate rheometer (RSA3, TA Instruments, New Castle, DE). The top plate was lowered at a speed of 0.0005 mm/s [inset Fig. 2(A)], and the force F and plate separation H were recorded as a function of time. Initially, the water in the film between the sample and solid plates is squeezed out. At some point, the water film becomes thin enough that the pressure within it is sufficient to deform the sample. A typical force versus time curve is shown in Figure 2(A). Figure 2(A) also shows the time at which the sample begins to deforms, t_0, and the initial sample thickness H_0. The latter was determined by assuming that the thickness of the water film between the sample and the plates was negligible. The Hencky strain, ε, was defined as follows:

$$\varepsilon = -0.5 \ln (H/H_0). \tag{1}$$

The sample volume was assumed constant so that the area of contact between the sample and the plate A could be determined as follows:

$$A = A_0 H_0 / H, \tag{2}$$

where

$$A_0 = (\pi/4) D_0^2. \tag{3}$$

The stress in the sample, σ, was obtained from:

$$\sigma = F/A. \tag{4}$$

At small strains ($\varepsilon \ll 1$), a plot of stress versus strain should be linear. As shown in Figure 2(B), a nonlinear

relationship is observed for $\varepsilon \leq 0.005$. The deviation from linear behavior is the result of the squeezing of the water film. In other words, there is a small error in estimating the initial sample thickness H_0. A revised estimate of H_0 was made, and the resulting stress versus strain plot is shown in Figure 2(B). The second estimate of the initial sample thickness is made from the point at which a linear stress versus strain is observed in Figure 2(B). This iterative procedure was continued until a linear stress–strain behavior was observed over the entire range of strains. The third (and final) iteration produced the results shown in Figure 2(C). The slope of the linear stress versus strain result was used to determine elastic modulus, E, from the relationship:

$$E = \sigma/\theta. \tag{5}$$

The analysis described above assumes the sample undergoes a uniform equibiaxial deformation, which implies that there is perfect slip between the sample and disk.

Statistical analysis

All the experiments were conducted three times with at least two replications per treatment. Four randomly selected regions per treatment were imaged and used to determine cell adhesion. This resulted in a data set with a minimum of 12 measurements for each treatment in an experiment. For the analysis of cell spreading, 60 randomly selected cells from each treatment were analyzed. A one-factor analysis of variance was used to statistically evaluate the effect of each treatment on cell attachment and spreading. A two-sided significance level of 5% was used for Student t tests when comparing the means of different treatments. p values ≤ 0.05 were considered statistically significant.

RESULTS AND DISCUSSION

Characterization of GST-III$_{9\text{-}10}$ and GRGDSPC conjugation to PEGDA by calorimetry

Our goal was to compare the effect of PEG hydrogels derivatized with different amounts of III$_{9\text{-}10}$ and GRGDSPC on cell spreading and adhesion. Because protein structure and function are inherently linked, we devised a strategy of conjugation that would result in minimal modification of III$_{9\text{-}10}$. We used a fusion of GST-III$_{9\text{-}10}$ for our studies. GST-III$_{9\text{-}10}$ is routinely produced from bacterial expression systems and then purified by GST-affinity chromatography.[21,24,25] GST has three accessible cysteine residues[14] and therefore three thiol groups for addition reactions, whereas III$_{9\text{-}10}$ has none[6]. We used Michael addition to tether GST-III$_{9\text{-}10}$ or GRGDSPC to PEGDA (Fig. 1). The RGD and III$_{9\text{-}10}$ groups formed pendant chains in the PEG hydrogel network. The control treatment consisted of a PEG hydrogel without bioconjugates.

Conjugation of PEG via the Michael addition strategy reduces the number of free thiols in solution. Therefore, thiol content can be used to monitor reaction kinetics. We reacted 1 μM of GRGDSPC or GST-III$_{9\text{-}10}$ with a more than 3000-fold molar excess of PEGDA and followed the kinetics of thiol consumption by Ellman's reagent.[26] A standard

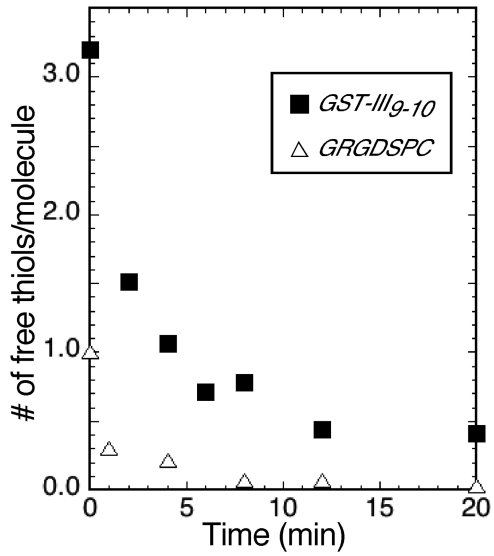

FIGURE 3. Kinetics of PEGDA conjugation to 1 μM GST-III$_{9\text{-}10}$ and GRGDSPC in PBS at 37°C. Error bars are not visible.

curve of cysteine monohydrate was used to convert absorbance readings to number of free thiols per molecule. Figure 3 shows the number of free thiols per molecule of GST-III$_{9\text{-}10}$ or GRGDSPC at different time points, after the addition of PEGDA. The zero time point in Figure 3 shows that the number of free thiols in GST-III$_{9\text{-}10}$ is three times that in GRGDSPC. This is in agreement with the amount of cysteine residues in the two molecules. Twenty minutes after the addition of PEGDA, 87 and 96% of the thiol groups in GST-III$_{9\text{-}10}$ and GRGDSPC, respectively, were conjugated to PEG. GRGDSPC was conjugated to PEG at a faster rate than GST-III$_{9\text{-}10}$. The differences in reaction rates between GRGDSPC and GST-III$_{9\text{-}10}$ can be attributed to the differences in their sizes: the molecular weight of GRGDSPC and GST-III$_{9\text{-}10}$ is 0.69 and 45 kDa, respectively. Thus, the smaller GRGDSPC molecule diffuses much faster than GST-III$_{9\text{-}10}$, resulting in higher reaction rates. The data were linearized to first-order kinetics, and the kinetic rate constants determined. The rate constants were obtained from the slope of the natural logarithm of the number of free thiols per molecule versus time. The first-order rate constants for PEG conjugation were 0.149 ($R^2 = 0.82$) and 0.093 ($R^2 = 0.76$) min^{-1} for GRGDSPC and GST-III$_{9\text{-}10}$, respectively. The kinetics of PEGDA conjugation to GRGDSPC are comparable to those reported by others.[27] The rate of conjugation of PEGDA to GST-III$_{9\text{-}10}$ is faster than that obtained by Ghosh et al.[11] for conjugation of III$_{7\text{-}10}$ with PEG divinyl sulfone. Moreover, our single-step approach of conjugating PEG to III$_{9\text{-}10}$ is more facile than the multistep strategy used by Ghosh et al.[11]

Characterization of PEGDA conjugation to GST-III$_{9\text{-}10}$ by SDS-PAGE

We examined the products of an extended reaction time between GST-III$_{9\text{-}10}$ and PEGDA by immunoblotting with antibodies that bind to III$_{9\text{-}10}$. GST-III$_{9\text{-}10}$ at concentrations

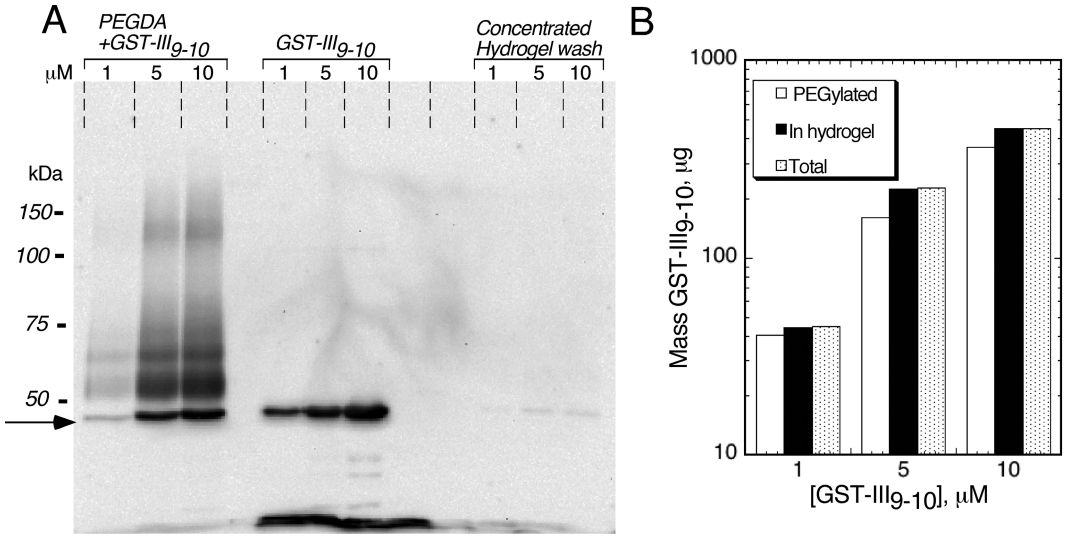

FIGURE 4. Characterization of the products of PEGDA conjugation to GST-III_{9-10} by immunoblotting with antibodies specific for III_{9-10}. (A) Immunoblot of products obtained from 1, 5, or 10 μM GST-III_{9-10} in 10% (wt/vol) PEGDA after 1 h at 37°C. The immunoblot also shows the control reaction consisting of 1, 5, and 10 μM GST-III_{9-10} mixed with an equal volume of PBS. The amount electrophoresed was 0.73 μL of the reaction mixture. The last three lanes represent 4.4 μL of a 40× concentrated wash solution of PEG hydrogels. Arrow = 45 kDa. (B) Densitometric quantification of GST-III_{9-10} in the immunoblot. Total is the amount of starting GST-III_{9-10}; PEGylated is the amount of GST-III_{9-10} conjugated to PEGDA = Total − 45 kDa band in PEGDA + GST-III_{9-10} lane; In hydrogel is the amount of GST-III_{9-10} in the hydrogel = Total − (40 × 45 kDa band in concentrated hydrogel wash).

of 1, 5, and 10 μM in 10% (w/v) PEGDA was incubated for 1 h at 37°C and then immunoblotted with antibodies that bind to III_{9-10}. Figure 4(A) shows an immunoblot of the products of the reaction between GST-III_{9-10} and PEGDA at different concentrations. It also shows control reactions comprising GST-III_{9-10} alone and GST-III_{9-10} in the wash solution of PEG hydrogels. There is an increase in the molecular weight of the bands in the lanes containing PEGDA and GST-III_{9-10} compared with the lane with GST-III_{9-10} alone, which indicates PEG conjugation. The bands with molecular weight higher than that of GST-III_{9-10} are smeared. We attribute this to the polydispersity of PEG.[28] The molecular weight of bands (i), (ii), and (iii) in Figure 4, calculated from a standard curve using commercially available protein standards, is 50–57, 62–64, and 117–128 kDa, respectively. The band at 117–128 kDa represents two GST-III_{9-10} molecules bound together by PEG. These values of molecular weight for bands (i), (ii), and (iii) correspond to three to six PEGDA molecules conjugated to GST-III_{9-10} and up to seven PEGDA molecules conjugated to two GST-III_{9-10} molecules. The expected values for the number of PEGDA molecules conjugated to GST-III_{9-10} and to a dimmer of GST-III_{9-10} are one to three and one to five, respectively. We attribute the difference between the expected and observed molecular weights of PEG-conjugated GST-III_{9-10} to branching in the polypeptide, which decreases electrophoretic mobility of the conjugate relative to the unmodified protein standards. This effect has been reported to lead to discrepancies in the expected and measured molecular weight of PEG-conjugated proteins.[29]

We increased GST-III_{9-10} concentration to determine whether there was saturation binding to PEG conjugation. The products of PEGDA conjugation to GST-III_{9-10} at concentrations of 1, 5, and 10 μM are shown in Figure 4(A). Band intensity associated with PEG-conjugated GST-III_{9-10} positively correlates with the amount of GST-III_{9-10} in the solution. We could not sample GST-III_{9-10} concentrations equal to or higher than 20 μM because the protein aggregated and precipitated from solution.

To verify the efficiency of PEGDA conjugation to GST-III_{9-10} obtained by calorimetry, and to determine how much of the starting material was immobilized in PEG hydrogels, we quantified the 45-kDa band in the immunoblots. This band corresponds to the molecular weight of GST-III_{9-10}. Figure 4(B) is a quantitative analysis of the blot in Figure 4(A). The amount of PEG-conjugated GST-III_{9-10} was determined by subtracting the intensity of the 45-kDa band in the lanes containing a mixture of GST-III_{9-10} and PEGDA from the lanes containing GST-III_{9-10} alone. The efficiency of PEGDA conjugation to 1 μM GST-III_{9-10} determined by densitometric analysis was 90.4%. This efficiency is comparable to that obtained by the kinetic rate constants obtained from calorimetry (Fig. 3). The efficiency of PEGDA conjugation to 5 and 10 μM GST-III_{9-10} was 71.3 and 80.2%, respectively. The amount of GST-III_{9-10} in the PEG hydrogel was determined from the intensity of the 45-kDa band in the concentrated hydrogel wash solution and correcting this intensity by the concentration factor. From the amount recovered in the wash solution, we determined that 98.7, 99.5, and 99.7% of 1, 5, and 10 μM, respectively, of the starting GST-III_{9-10} was present in the PEG hydrogel. These results demonstrate that additional conjugation of PEGDA to GST-III_{9-10} may occur during hydrogel formation or GST-III_{9-10} may be trapped in the hydrogel network.

Limited proteolysis and CD studies of PEG-conjugated GST-III_{9-10}

The site of PEG conjugation and the size of the PEG molecule may influence the structure of the protein[30] and

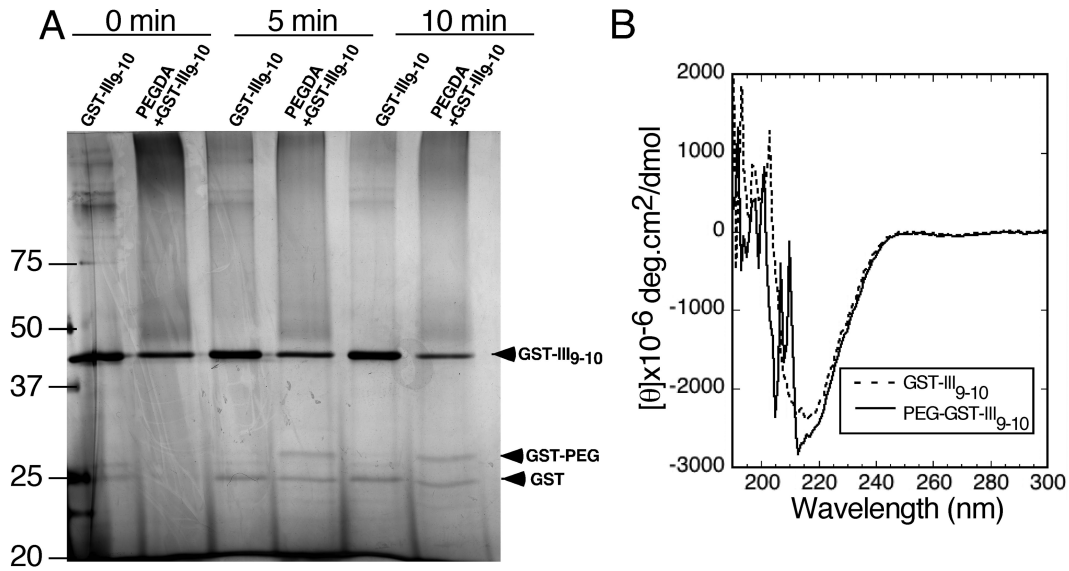

FIGURE 5. Characterization of PEG-conjugated GST-III_{9-10} by proteolysis and CD. (A) SDS-PAGE analysis of the silver-stained products formed after limited proteolysis of PEG-conjugated GST-III_{9-10} and GST-III_{9-10}. Molecular weight standards are shown on the left, and the arrows on the right mark the products of proteolysis. (B) CD spectra of GST-III_{9-10} and PEG-conjugated GST-III_{9-10} (PEG-GST-III_{9-10}) in PBS.

subsequently its function. We used limited proteolysis and CD studies to determine whether there were major structural changes to GST-III_{9-10} after PEG conjugation. Limited proteolysis and CD studies have been used extensively to characterize protein folding.[31–34] We added α chymotrypsin, which cleaves between fibronectin modules,[15] to native and PEG-conjugated GST-III_{9-10} and characterized the products of proteolysis by SDS-PAGE. Figure 5(A) shows the products of α chymotrypsin proteolysis 5–10 min after protease addition. It is important to note that the lane with PEG-conjugated GST-III_{9-10} contains a 45-kDa band, which corresponds to unconjugated GST-III_{9-10}. Addition of α chymotrypsin results in a 25-kDa band in both treatments, which is the molecular weight of GST. In the lane containing GST-III_{9-10} conjugated to PEG, a 28-kDa band is clearly visible for 5–10 min after the addition of α chymotrypsin. The molecular weight of this band corresponds to the molecular weight of GST and PEGDA combined. Therefore, α chymotrypsin cleaves between GST and III_{9-10} in the native and PEG-conjugated protein. Figure 5(B) shows the molar ellipticities of native and PEG-conjugated GST-III_{9-10}. GST is an α/β protein with a dominant α signal,[35] whereas the predominant secondary structure elements in III_{9-10} are β-sheets.[6] Significant changes in the structure of the PEG-conjugated GST-III_{9-10} would result in changes in the shape and intensity of the absorption spectra. The percentage difference in ellipticity of native and PEG-conjugated GST-III_{9-10} was obtained at each wavelength and integrated between 217 and 300 nm to obtain an average value. The average percentage difference in the ellipticity of the native and PEG-conjugated GST-III_{9-10} was 7.74%. Light scattering below a wavelength of 217 nm is significant (the dynode voltage is greater than 600 V) and results in fluctuation in the ellipticities of both the native and PEG-conjugated GST-III_{9-10}. The CD and limited proteolysis studies demonstrate that our approach of conjugating PEGDA to GST-III_{9-10} does not significantly perturb the structure of GST-III_{9-10}.

Effect of PEG hydrogels conjugated with GST-III_{9-10} and GRGDSPC on cell adhesion and spreading

We examined the effect of PEG hydrogels functionalized with GST-III_{9-10} or GRGDSPC on cell adhesion and spreading. Varying concentrations of PEG-conjugated GST-III_{9-10} or GRGDSPC were mixed with PEGDA and initiator and photopolymerized to form the functionalized PEG hydrogels. The highest concentration of GRGDSPC selected matches the concentration of RGD that has been used by others.[2,3,36] NIH-3T3 mouse embryonic fibroblasts were cultured on functionalized surfaces in a serum-free environment to eliminate the contribution of growth factors and other ECM proteins in serum on cell adhesion. Figure 6(A) shows fluorescence images of NIH-3T3 mouse embryonic fibroblasts cultured on functionalized PEG hydrogels. Increasing GST-III_{9-10} or GRGDSPC concentration corresponded to higher cell adhesion and spreading. Figure 6(A) shows that the number of cells on hydrogels with 1 μ*M* GST-III_{9-10} is greater than those on 1 μ*M* RGD-functionalized PEG hydrogels. Figure 6(B,C) represents a quantitative analysis of cell adhesion and spreading on the functionalized PEG hydrogels. There is statistically significant higher attachment and spreading on the hydrogels functionalized with 1 μ*M* GST-III_{9-10} than on the 1 μ*M* GRGDSPC-functionalized PEG hydrogels. It is important to note that robust cell responses that have been reported on RGD-functionalized PEG hydrogels used solution peptide concentrations on the millimolar range.[2,3,36] Cell attachment and spreading on PEG hydrogels with 1 μ*M* GST-III_{9-10} is comparable to that on 500 μ*M* GRGDSPC. On a molar basis, PEG hydrogels derivatized with GST-III_{9-10} provide a more robust response than hydrogels derivatized with GRGDSPC. These studies on compliant

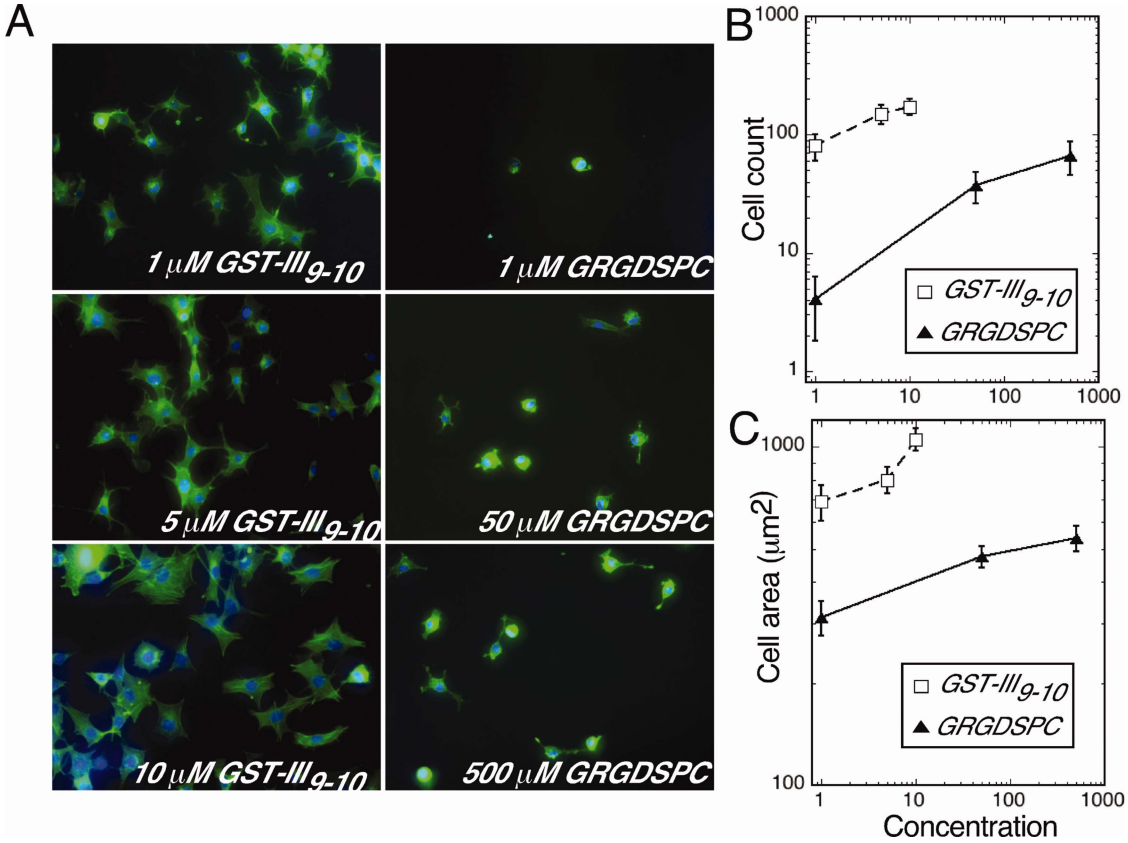

FIGURE 6. Comparison of cell attachment and spreading on PEG hydrogels tethered with 1–10 μ*M* GST-III$_{9\text{-}10}$ and 1–500 μ*M* GRGDSPC. (A) Images of cells captured after culture in serum-free media on functionalized PEG hydrogels. Nuclei and actin have been stained blue (Hoechst) and green (phalloidin-fluorescein), respectively. (B) Cell count and (C) cell spreading on functionalized PEG hydrogels. The error bars in (B) and (C) represent a 95% confidence interval of the standard errors of the mean. The data were obtained from two replicates and three different experiments. [Color figure can be viewed in the online issue, which is available at wileyonlinelibrary.com.]

scaffolds are extension of the findings by Petrie et al.[10] on RGD and III$_{7\text{-}10}$ immobilization on rigid gold surfaces. The current work also builds on the findings of Ghosh et al.[11] on derivatized hydrogels while examining the effect of PEG conjugation on III$_{9\text{-}10}$ structure. Another novelty of our study is that the bioconjugates in our study are present in the polymer networks as opposed to a planar surface and as such have the potential to modulate the mechanical properties of the polymer.

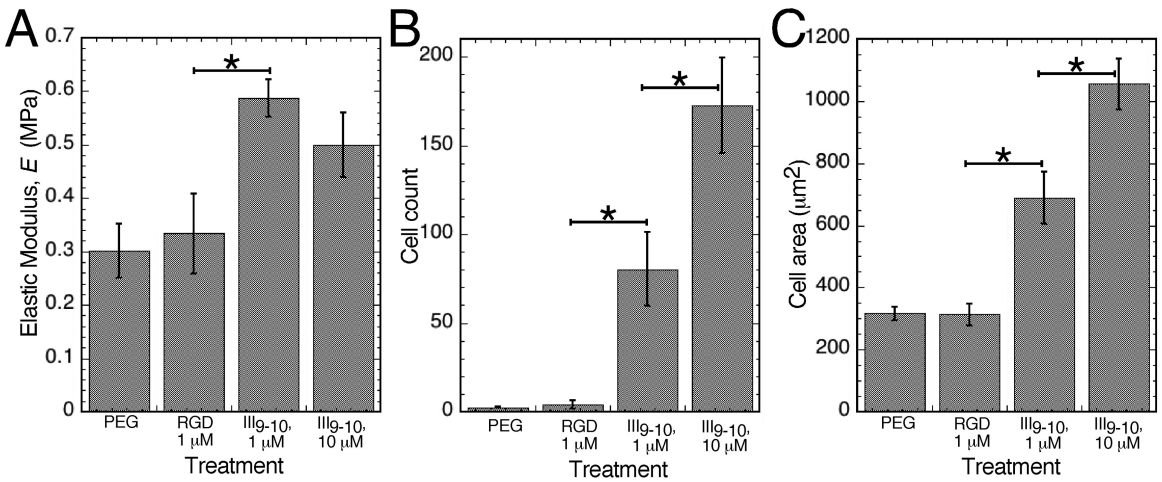

FIGURE 7. Elastic moduli of derivatized PEG hydrogels. (A) Elastic modulus, *E*, of PEG hydrogels without any conjugate (PEG) and with 1 μ*M* GRGDPSC (RGD 1 μ*M*), 1 μ*M* GST-III$_{9\text{-}10}$ (III$_{9\text{-}10}$ 1 μ*M*), and 10 μ*M* GST-III$_{9\text{-}10}$ (III$_{9\text{-}10}$ 10 μ*M*). (B) Cell adhesion and (C) cell spreading on derivatized PEG hydrogels with *E* values reported in (A). '*' represents a statistically significant difference in the mean.

Effect of GST-III$_{9\text{-}10}$ and GRGDSPC on PEG hydrogel rigidity

The presence of bioconjugates in hydrogels can have an effect on substrate rigidity, and significant changes in substrate rigidity influence biological responses such as cell adhesion and spreading.[13,37,38] Controlled compression studies were conducted to determine the elastic modulus of PEG hydrogels containing 1 μM GRGDSPC, 1 μM GST-III$_{9\text{-}10}$, and 10 μM GST-III$_{9\text{-}10}$ and control PEG hydrogels without any ligand. PEG hydrogels containing 1 μM GST-III$_{9\text{-}10}$ had a significantly higher elastic modulus than those without any conjugate or those conjugated to 1 μM GRGDSPC [Fig. 7(A)]. An increase in substrate rigidity positively correlated with cell spreading.[37,39] PEG hydrogels derivatized with 1 μM GRGDSPC had lower cell spreading and adhesion than those derivatized with 1 μM GST-III$_{9\text{-}10}$ [Figs. 6 and 7(B,C)]. Nevertheless, on the basis of the work by Peyton et al., the differences in the elastic moduli of GST-III$_{9\text{-}10}$- and GRGDSPC-derivatized hydrogels are not large enough to result in the differences observed in cell spreading. They reported that an increase of 0.5 MPa in the elastic modulus of RGD-derivatized PEG hydrogels resulted in a 14% increase in smooth muscle cell spreading. GRGDSPC- and GST-III$_{9\text{-}10}$-derivatized PEG hydrogels have a 0.25-MPa difference in their elastic moduli, but a twofold change in spreading area. This change in spreading is significantly higher than would be present if the responses were based solely on substrate rigidity. Moreover, increasing the concentration of GST-III$_{9\text{-}10}$ from 1 to 10 μM in PEG hydrogels does not have a significant effect on elastic modulus but results in a significant increase in cell spreading and adhesion [Fig. 7(B,C)]. On a molar basis, GST-III$_{9\text{-}10}$ chemistry stimulates a significantly more robust biological response than GRGDSPC chemistry. In addition, the effect of substrate rigidity is negligible compared with the effects of conjugated chemistries in the GST-III$_{9\text{-}10}$- and GRGDSPC-derivatized PEG hydrogels.

CONCLUSION

We demonstrate covalent bonding between the cell-binding domain of fibronectin, III$_{9\text{-}10}$, and a PEG hydrogel through a GST affinity tag. This method of PEG conjugation through a GST affinity tag is novel, rapid, and efficient and produces a scaffold with a well-defined chemistry. Scaffolds functionalized with III$_{9\text{-}10}$ stimulate more robust cell adhesion and spreading than RGD-functionalized PEG hydrogels. We demonstrate that, although there are differences in rigidity between III$_{9\text{-}10}$ and RGD-functionalized PEG hydrogels, the biological cues from GST-III$_{9\text{-}10}$ are more dominant with respect to cell spreading and adhesion. In addition to the cell-binding domain, there are fibronectin- and heparin-binding domains in the type III repeats that (i) are cysteine free or have cysteine residues buried in the core of the domain,[40] (ii) can be expressed as GST-fusion proteins, and (iii) can be immobilized on PEG hydrogels using our approach. Therefore, our method may be used to develop PEG hydrogel scaffolds with multiple functionalities.

REFERENCES

1. Zhu J. Bioactive modification of poly(ethylene glycol) hydrogels for tissue engineering. Biomaterials 2010;31:4639–4656.
2. Burdick JA, Anseth KS. Photoencapsulation of osteoblasts in injectable RGD-modified PEG hydrogels for bone tissue engineering. Biomaterials 2002;23:4315–4323.
3. Hahn MS, McHale MK, Wang E, Schmedlen RH, West JL. Physiologic pulsatile flow bioreactor conditioning of poly(ethylene glycol)-based tissue engineered vascular grafts. Ann Biomed Eng 2007;35:190–200.
4. Mendez MV, Stanley A, Park HY, Shon K, Phillips T, Menzoian JO. Fibroblasts cultured from venous ulcers display cellular characteristics of senescence. J Vasc Surg 1998;28:876–883.
5. Aota S, Nomizu M, Yamada KM. The short amino acid sequence Pro-His-Ser-Arg-Asn in human fibronectin enhances cell-adhesive function. J Biol Chem 1994;269:24756–24761.
6. Leahy DJ, Aukhil I, Erickson HP. 2.0 A crystal structure of a four-domain segment of human fibronectin encompassing the RGD loop and synergy region. Cell 1996;84:155–164.
7. Altroff H, Schlinkert R, van der Walle CF, Bernini A, Campbell ID, Werner JM, Mardon HJ. Interdomain tilt angle determines integrin-dependent function of the ninth and tenth FIII domains of human fibronectin. J Biol Chem 2004;279:55995–56003.
8. Ochsenhirt SE, Kokkoli E, McCarthy JB, Tirrell M. Effect of RGD secondary structure and the synergy site PHSRN on cell adhesion, spreading and specific integrin engagement. Biomaterials 2006; 27:3863–3874.
9. Martino MM, Mochizuki M, Rothenfluh DA, Rempel SA, Hubbell JA, Barker TH. Controlling integrin specificity and stem cell differentiation in 2D and 3D environments through regulation of fibronectin domain stability. Biomaterials 2009;30:1089–1097.
10. Petrie TA, Capadona JR, Reyes CD, Garcia AJ. Integrin specificity and enhanced cellular activities associated with surfaces presenting a recombinant fibronectin fragment compared to RGD supports. Biomaterials 2006;27:5459–5470.
11. Ghosh K, Ren XD, Shu XZ, Prestwich GD, Clark RA. Fibronectin functional domains coupled to hyaluronan stimulate adult human dermal fibroblast responses critical for wound healing. Tissue Eng 2006;12:601–613.
12. Cosson S, Kobel SA, Lutolf MP. Capturing complex protein gradients on biomimetic hydrogels for cell-based assays. Adv Funct Mater 2009;19:3411–3419.
13. Engler AJ, Humbert PO, Wehrle-Haller B, Weaver VM. Multiscale modeling of form and function. Science 2009;324:208–212.
14. McTigue MA, Williams DR, Tainer JA. Crystal structures of a schistosomal drug and vaccine target: Glutathione S-transferase from *Schistosoma japonica* and its complex with the leading antischistosomal drug praziquantel. J Mol Biol 1995;246:21–27.
15. Lutolf MP, Tirelli N, Cerritelli S, Cavalli L, Hubbell JA. Systematic modulation of Michael-type reactivity of thiols through the use of charged amino acids. Bioconjug Chem 2001;12:1051–1056.
16. Friedman M, Cavins JF, Wall JS. Relative nucleophilic reactivities of amino groups and mercaptide ions in addition reactions with α,β-unsaturated compounds. J Am Chem Soc 1965;87:3672–3682.
17. Elbert DL, Hubbell JA. Conjugate addition reactions combined with free-radical cross-linking for the design of materials for tissue engineering. Biomacromolecules 2001;2:430–441.
18. Cruise GM, Scharp DS, Hubbell JA. Characterization of permeability and network structure of interfacially photopolymerized poly(ethylene glycol) diacrylate hydrogels. Biomaterials 1998;19:1287–1294.
19. Salinas CN, Anseth KS. Decorin moieties tethered into PEG networks induce chondrogenesis of human mesenchymal stem cells. J Biomed Mater Res 2009;90:456–464.
20. Chiang C, Karuri SW, Kshatriya PP, Schwartz J, Schwarzbauer J, Karuri NW. A surface derivatization strategy for combinatorial analysis of cell response to mixtures of protein domains. Langmuir 2012;28:548–556.
21. Kshatriya PP, Karuri SW, Chiang C, Karuri NW. A combinatorial approach for directing the amount of fibronectin fibrils assembled by cells that uses surfaces derivatized with mixtures of fibronectin and cell binding domains. Biotechnol Prog 2012;28:862–871.
22. Bryant SJ, Bender RJ, Durand KL, Anseth KS. Encapsulating chondrocytes in degrading PEG hydrogels with high modulus:

Engineering gel structural changes to facilitate cartilaginous tissue production. Biotechnol Bioeng 2004;86:747–755.
23. Terraciano V, Hwang N, Moroni L, Park HB, Zhang Z, Mizrahi J, Seliktar D, Elisseeff J. Differential response of adult and embryonic mesenchymal progenitor cells to mechanical compression in hydrogels. Stem Cells 2007;25:2730–2738.
24. Hocking DC, Chang CH. Fibronectin matrix polymerization regulates small airway epithelial cell migration. Am J Physiol Lung Cell Mol Physiol 2003;285:L169–L179.
25. Sechler JL, Takada Y, Schwarzbauer JE. Altered rate of fibronectin matrix assembly by deletion of the first type III repeats. J Cell Biol 1996;134:573–583.
26. Ellman GL. A colorimetric method for determining low concentrations of mercaptans. Arch Biochem Biophys 1958;74:443–450.
27. Salinas CN, Anseth KS. Mixed mode thiol-acrylate photopolymerizations for the synthesis of PEG-peptide hydrogels. Macromolecules 2008;41:6019–6026.
28. Veronese FM. Peptide and protein PEGylation: A review of problems and solutions. Biomaterials 2001;22:405–417.
29. Kurfurst MM. Detection and molecular weight determination of polyethylene glycol-modified hirudin by staining after sodium dodecyl sulfate-polyacrylamide gel electrophoresis. Anal Biochem 1992;200:244–248.
30. Grace MJ, Lee S, Bradshaw S, Chapman J, Spond J, Cox S, Delorenzo M, Brassard D, Wylie D, Cannon-Carlson S, Cullen C, Indelicato S, Voloch M, Bordens R. Site of pegylation and polyethylene glycol molecule size attenuate interferon-alpha antiviral and antiproliferative activities through the JAK/STAT signaling pathway. J Biol Chem 2005;280:6327–6336.
31. Karuri NW, Lin Z, Rye HS, Schwarzbauer JE. Probing the conformation of the fibronectin III1-2 domain by fluorescence resonance energy transfer. J Biol Chem 2009;284:3445–3452.
32. Pavone LM, Del Vecchio P, Mallardo P, Altieri F, De Pasquale V, Rea S, Martucci NM, Di Stadio CS, Pucci P, Flagiello A, Masullo M, Arcari P, Rippa E. Structural characterization and biological properties of human gastrokine 1. Mol Biosyst 2013;9:412–421.
33. Roman EA, Faraj SE, Gallo M, Salvay AG, Ferreiro DU, Santos J. Protein stability and dynamics modulation: The case of human frataxin. PLoS One 2012;7:e45743.
34. Wennerstrand P, Dametto P, Hennig J, Klingstedt T, Skoglund K, Appell ML, Martensson LG. Structural characteristics determine the cause of the low enzyme activity of two thiopurine S-methyltransferase allelic variants: A biophysical characterization of TPMT*2 and TPMT*5. Biochemistry 2012;51:5912–5920.
35. Masino L, Kelly G, Leonard K, Trottier Y, Pastore A. Solution structure of polyglutamine tracts in GST-polyglutamine fusion proteins. FEBS Lett 2002;513:267–272.
36. Hern DL, Hubbell JA. Incorporation of adhesion peptides into non-adhesive hydrogels useful for tissue resurfacing. J Biomed Mater Res 1998;39:266–276.
37. Peyton SR, Raub CB, Keschrumrus VP, Putnam AJ. The use of poly(ethylene glycol) hydrogels to investigate the impact of ECM chemistry and mechanics on smooth muscle cells. Biomaterials 2006;27:4881–4893.
38. Engler AJ, Griffin MA, Sen S, Bonnemann CG, Sweeney HL, Discher DE. Myotubes differentiate optimally on substrates with tissue-like stiffness: Pathological implications for soft or stiff microenvironments. J Cell Biol 2004;166:877–887.
39. Lo CM, Wang HB, Dembo M, Wang YL. Cell movement is guided by the rigidity of the substrate. Biophys J 2000;79:144–152.
40. Pankov R, Yamada KM. Fibronectin at a glance. J Cell Sci 2002; 115:3861–3863.